Supplemental Materials

Molecular Biology of the Cell

Miroshnikova et al.

Supplemental Information

A rigid extracellular matrix promotes malignancy by enhancing $\alpha5\beta1$ integrin ligation of the fibronectin synergy site and vinculin and zyxin recruitment and PI3 kinase activation

***Miroshnikova, Y.A., *Rozenberg, G.I.,*Cassereau, L., Pickup, M., Mouw, J.K., Ou, G, Templeman, K.L., Elloumi-Hannachi, I., Gooch, K., Sarang- Sieminski, A.L., García, A.J., Weaver V.M.**

*Denotes equal contribution

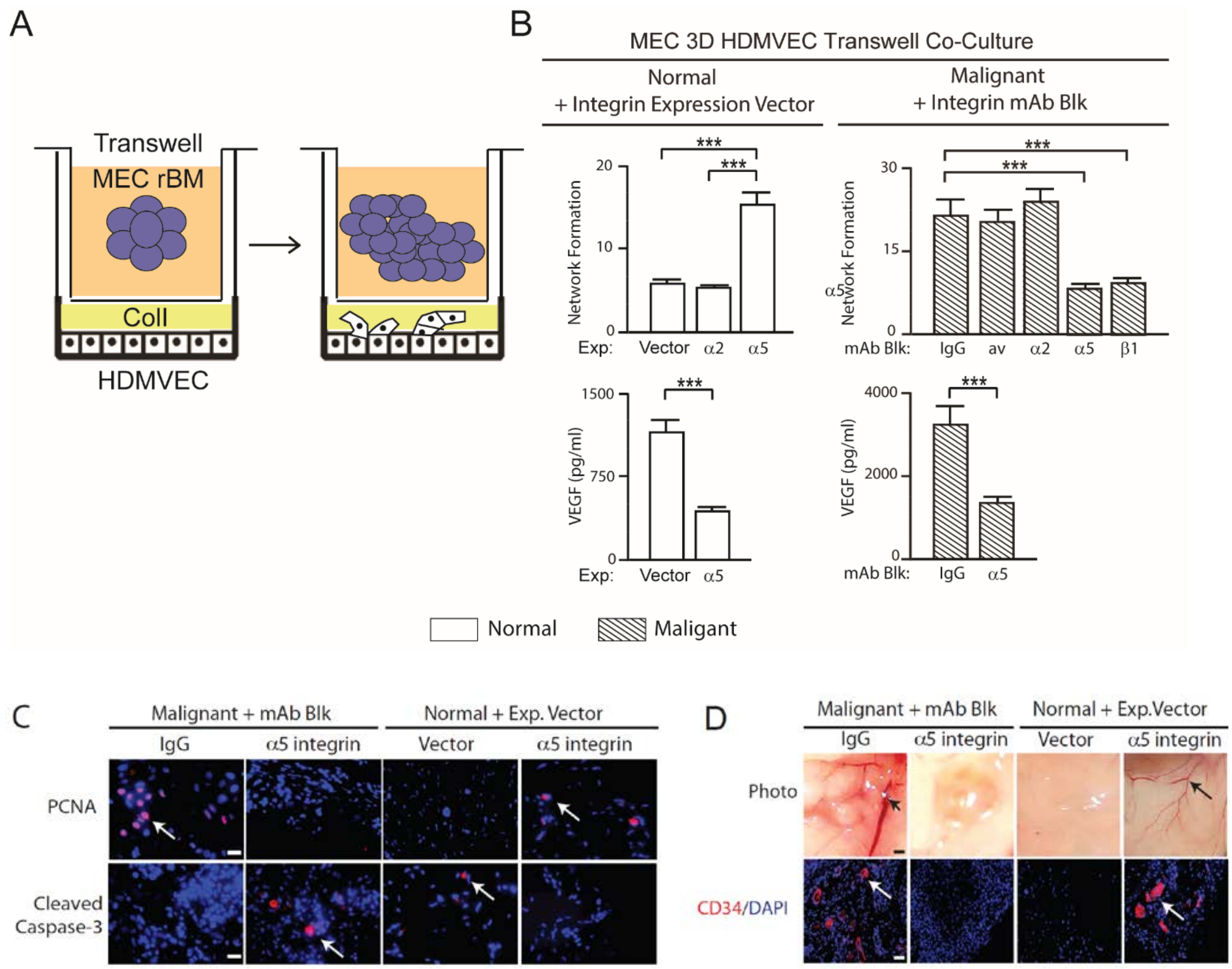

Figure S1. α5β1 integrin expression promotes angiogenesis and VEGF secretion in vitro and in vivo. A) Schematic of an *in vitro* endothelial network formation model system by human dermal microvascular endothelial cells (HDMVECs) co-cultured with MECs. B) *In vitro* network formation of HDMVECs is (top left) greatly increased in a co-culture setting with non-malignant MECs over-expressing α5 integrin and is (top right) highly reduced when either β1 or α5 integrins are functionally-blocked in the malignant MECs, but not α2 or αv; (bottom left) nonmalignant MECs overexpressing α5 integrin secrete higher levels of VEGF and (bottom right) function-blocking of α5 integrin in malignant MECs reduces their VEGF. **C)** Immunofluorescence images of xenograft mouse tissues stained for PCNA (top) and activated caspase 3 (lower). Scale Bar 10 µm. **D)** (upper panel) Photomicrographs of vasculature in tissue from injected malignant T4-2 MECs with and without α5 integrin inhibition and nonmalignant S-1 MECs expressing empty vector or elevated α5 integrin. Scale Bar 10 mm. (lower panel) Immunofluorescence images of xenograft mouse tissue stained for the endothelial marker CD34. Results are the mean ± S.E.M. of 3 separate experiments (***$p < 0.001$).

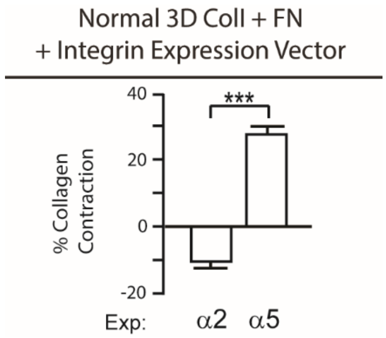

Figure S2. MECs overexpressing α5β1 integrin are highly contractile. Nonmalignant MECs overexpressing α5 integrin are able to contract 3-dimensional collagen gels to a much greater extent than those overexpressing α2 integrin. Results are the mean ± S.E.M. of 3 separate experiments (***$p < 0.001$).

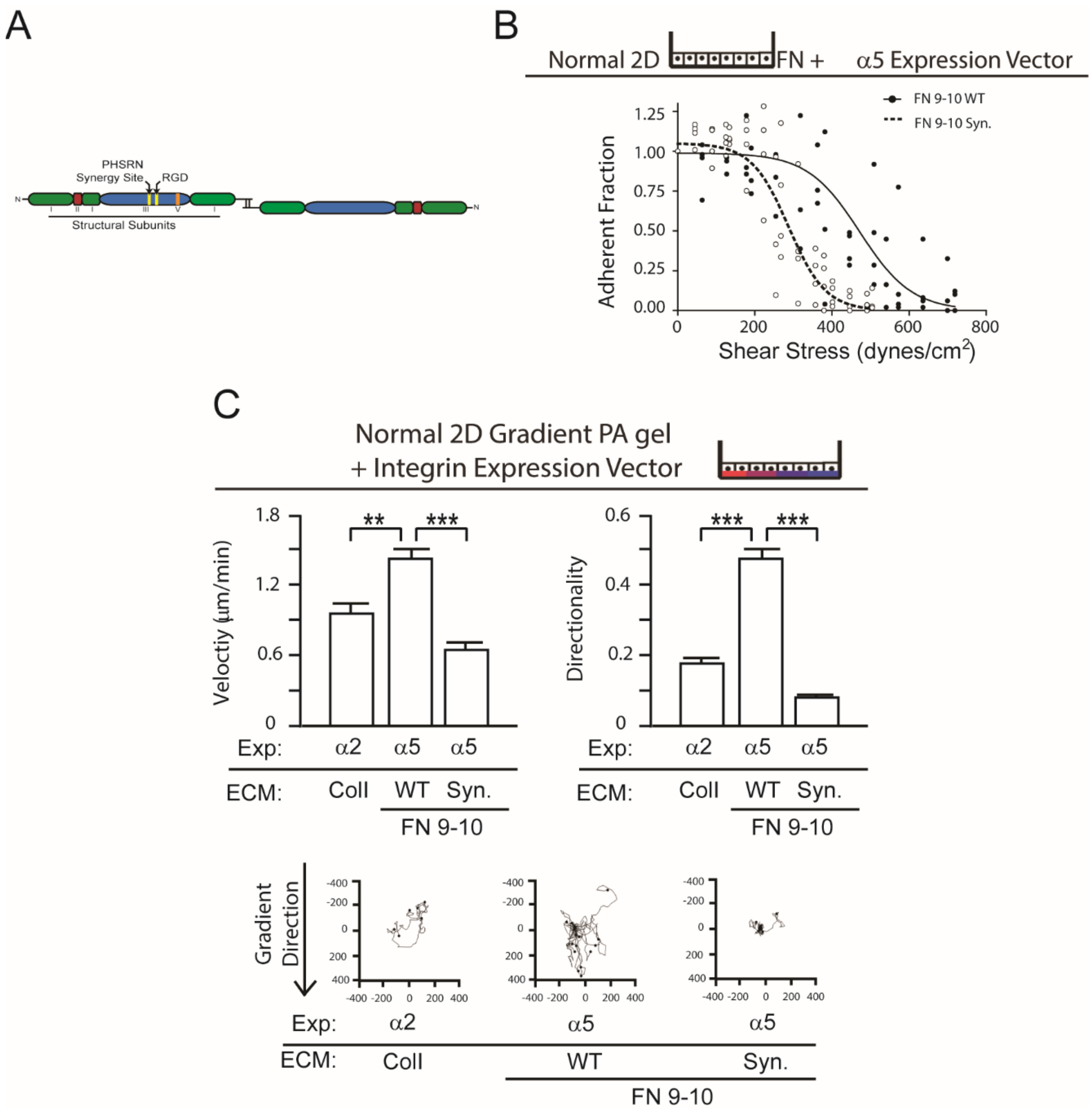

Figure S3. α5β1 integrin's interaction with fibronectin is mechano-sensitive and mechano-responsive. A) Schematic of FN domains relating RGD position to synergy site position. α5β1 integrin is able to switch between relaxed and tensioned states and the switch is controlled through the engagement of the synergy site on the fibronectin under high tension environments. The schematic represents the relative positions of the RGD and the synergy sites on the fibronectin's type III domain. **B)** Higher fraction of MECs overexpressing α5 integrin remained adherent to WT versus synergy-site mutated FN9-10 with linearly increased applied hydrodynamic fluid shear force. **C)** Top: nonmalignant MECs overexpressing α5 integrin plated on wild type FN9-10 exhibit highly directional and fast migration towards the stiffer substrates when plated on polyacrylamide gels (PA) of gradient stiffness (140-60,000 Pa); this phenotype is abolished if the same cells are plated on FN9-10 with mutated synergy site. Bottom: images illustrate representative cell migration paths of MECs overexpressing α2 integrin migrating on collagen-coated PA gels of gradient stiffness as well as MECS overexpressing α5 integrin migrating on either WT or synergy-site-mutated FN9-10-coated PA gels of gradient stiffness.

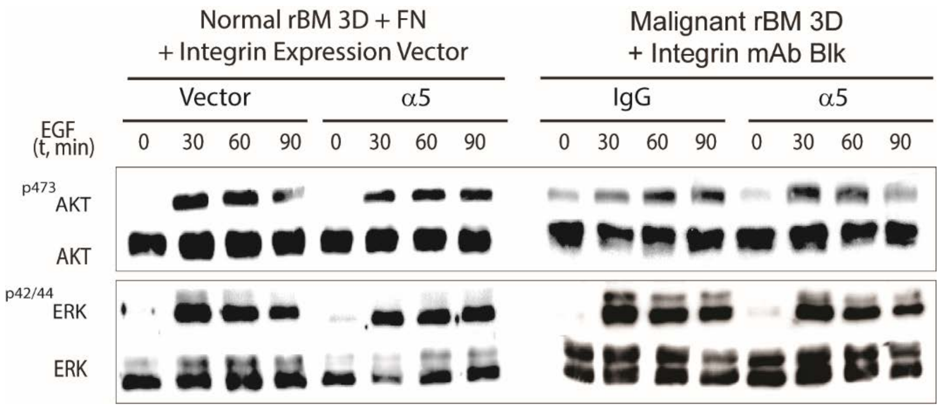

Figure S4. α5β1 potentiates sustained Erk and Akt signaling. Left: non-malignant MECs overexpressing α5 integrin exhibit sustained Erk and Akt signaling post EGF-stimulation after starvation. Right: function-blocking α5 integrin reduces the duration and potency of Erk and Akt signaling in malignant MECs.

Supplemental Experimental Procedures

Antibodies and reagents

The following primary antibodies were used for our studies: collagen IV, CIV 22, PCNA, and PC10 (DAKO); laminin-5 3-chain specific, BM165 (gift from Dr. Marinkovich); β1-integrin, AIIB2 (Dr. Damsky); TS2/16 (ATCC); β4 integrin 3E1, ASC-3, ASC-8; α1 integrin FB12, α2 integrin 10G11, α4 integrin P1H4, α5 integrin SAM-1 and P1D6, α6 integrin GoH3, αv integrin M9, fibronectin, 3E3, E-cadherin, vinculin (Chemicon International); pAkt substrate, pMLCK Thr18/Ser19, YAP, activated caspase 3 (Cell Signaling); pMypt Thr850 (Millipore), pFak Tyr397 (Invitrogen), Ki-67, β-catenin, Akt and pSer472/473/474-Akt, Erk1 (BD Transduction Laboratories); p-Erk1/2 (Thr202/Tyr204) (New England BioLabs); Flt-1/VEGFR1 Ab-1 (NeoMarkers). Phalloidin and anti-mouse/rabbit/rat IgG secondary antibodies, conjugated with FITC, Texas Red (Jackson Laboratories), AlexaFluor 488/555/647 (Invitrogen), and HRP (Amersham Pharmacia Biotech), were used. Inhibitors used were: EGFR-specific tyrosine kinase Tyrphostin AG 1478 (200 nM), MEK1: PD98059 (20 μM) and PI3 kinase LY 294002 (20 μM) (BIOMOL), fibronectin synergy site inhibitor (50 μM; gift from Dr. Mazar). In addition, the following proteins were utilized: fibronectin synergy site mutants (gift from H.P. Erickson), human recombinant VEGF Receptor 1 Flt-1 (Oncogene), and RGD peptide (Biomol International).

Cell Culture

Phenotypic reversion of T4-2 cells was as described [1]. To inhibit integrin function the 3D multicellular structures were pre-incubated with anti- α2, α5, or αv integrin-blocking antibodies or IgG isotype matched control mAb (20 g IgG/ml). Colony size and morphology were measured after 10-12 days in culture. Adult human dermal microvascular endothelial cells (HDMVECs) were grown on collagen type I-coated flasks (Collaborative Biomedical) in EGM-2 bullet kit media (Bio-Whitaker). Angiogenesis induction by MECs was assayed by co-culturing 3D rBM generated mammary organoids in cell culture inserts (0.45 m pore size; Biocoat, BD Labware) with HDMVECs that had been overlaid with a 1-mm-layer of acellular collagen type I (BD Pharmingen). HDMECs invasion through the collagen overlay and network formation was assessed after 2 days by staining with toluidine blue. Anchorage-independent growth was assessed using a soft agar assay [2]. Briefly, 20,000 cells in 1.0 ml 0.35% agarose with or without integrin blocking antibodies, as indicated, were overlaid with 1.0 ml 0.5% agarose containing 1X growth media, and colonies larger than 40 μm in diameter were scored positive after 21 days.

Western and ELISA Procedures

Equal amounts of cell protein lysate (either RIPA or Laemmli lysate; BCA; Pierce) were separated on reducing SDS-PAGE gels, transferred to nitrocellulose or PVDF membranes, and probed with primary antibody. Bands were visualized and quantified using a Fujifilm Gel Documentation system, in combination with HRP-conjugated secondary antibodies and ECL-Plus system (Amersham Pharmacia). Specific activity for Akt and Erk was calculated by normalizing densitrometric values of phosphorylated to total AKT or ERK and E-cadherin. Integrin protein levels were assessed using non-reducing SDS-PAGE gels. VEGF, Il-8 and bFGF levels in the media of 10-12 day three dimensional rBM cultures of MECs were measured using sandwich ELISA (R&D systems), according to the manufacturer's instructions. O.D. measurements were performed using a Fluoroskan Ascent FL (Labsystems).

RT PCR Primers

The following primer sequences were used: 18S: forward 5'- cggctaccacatccaaggaa-3', reverse 5'- gctggaattaccgcggct-3'; Fibronectin 1: forward 5'- agtgggagacctcgagaag-3, reverse 5'- gtccctcggaacatcagaaa-3', 5'-agtgggagacctcgagaag-3, reverse 5'- gtccctcggaacatcagaaa-3', VEGF: forward 5'- caggctgcacccatggcagaa-3', reverse 5'- gcatcgcatcaggggcacaca-3'.; ITGB1: forward 5'- cgaggtcatggttcatgttg -3', reverse 5'- tcccatttggcattcatttt-3'; ITGA5: forward 5'- agcctcagaaggaggaggac-3', reverse 5'- ggttaatggggtgattggtg-3', ITGA2 forward 5'- tgaccaaattctgcaggaca-3', reverse 5'- ggagccaatctggtcacct-3'; ITGAV forward 5'- ccaccaagctttggctattc-3', reverse 5'- caggcagtgagcaggtttta-3'.

Cell and Tissue Staining

3D rBM gels, as well as tissue sections, were prepared by mixing cultures with fresh collagen following embedment and freezing in sucrose with Tissue-Tek OCT compound (Miles Laboratories), then sectioned in 10-20 μm thick slices for analysis. All samples were incubated with primary mAbs followed directly by either FITC-, Texas red-, or AlexaFluor- conjugated secondary Abs. Nuclei were counterstained with diaminophenyl- indole (Sigma). Images were compared and quantified based on fluorescence intensity signal following minimal thresholding to subtract background. For mouse studies, when mice were sacrificed, lesions were photographed, dissected, measured, macroscopically analyzed, fixed in 4% paraformaldehyde, and paraffin embedded. H&E sections were evaluated for histopathological evidence of tumor phenotype and tissue sections were analyzed by immunofluorescence as described.

PA gel preparation Details

ECM-crosslinked PA gels were prepared and mechanically analyzed as described; single stiffness substrates [3] and mechanically gradient substrates [4]. Briefly, two droplets, each containing 12.5 μl of a soft (100 Pa) or stiff (60,000 Pa) acrylamide/bis-acrylamide mixture, are placed adjacent to each other on a large hydrophobic coverglass (no. 1, 45 mm × 50 mm; Fisher Scientific) and then covered with a small circular activated coverglass (no. 1, 18-mm diameter; Fisher Scientific) to merge the drops. By carefully maintaining the interface, a uniform gradient of 3.33Pa/um along the length of substrate is achieved. Regions of different rigidities were distinguished by using a fluorescently labeled bis-acrylamide in the stiff solution creating a gradient of fluorescence correlated with the mechanical gradient.

Substrate elastic modulus was measured via atomic force microscopy (Asylum Research) using the Hertz model [5]. Briefly, a silicon beaded tip cantilever (5um diameter, 0.07 N/m, silicon nitride) was used to measure 90 μm by 90 μm elastic modulus maps down the length of the gel along the mechanical gradient while simultaneously measuring fluorescence intensity with a inverted epi-fluorescence microscope. We used these measurements to assess the mechanical gradient and also develop an algorithm for determining the elastic modulus of the gel from solely the fluorescent intensity. This model allowed us to determine the particular surface stiffness seeded cells were adhered to when tracking cell motility.

Microscopy Setup

Immunofluorescence and FRET images were acquired using an Olympus IX81 Epifluorescence microscope with Spot color CCD camera, Nikon TE2000-U inverted microscope, Bio-Rad MRC 1024 laser scanning confocal microscope attached to a Nikon Diaphot 200 microscope, and a spinning disc/TIRF microscope setup with Andor's iXon3 EMCCD camera with the Yokogawa CSU-X1 confocal scanner, a Nikon TIRF illuminator, and a MOSAIC module for FRAP and photo-activation on a motorized Nikon Ti-E inverted microscope base.

Adhesion Strength Assay and Generation of Recombinant Fibronectin

Preparation of adhesive ligands: the previously described Promega Pinpoint vector containing the sequence for a fragment spanning the 7^{th} to 10^{th} type III repeat of human fibronectin (FN7-10) [6] was cut with NruI and ligated to yield an expression vector for a fragment spanning the 9^{th} to 10^{th} type III repeat of human fibronectin (FN9-10). The synergy site mutant PHSAN (FN9-10(PHSAN)) was generated using the Stratagene QuikChange Site Directed Mutagenesis kit and primers 5'-GGGTGCCCCACTCTGCGAATTCCATCACCC-3' (forward) and 5'-GGGTGATGGAATTCGCAGAGTGGGGCACCC-3' (reverse). Constructs were verified by DNA sequencing. Proteins were expressed in JM109 cells (Promega) in the presence of d-biotin and purified by affinity chromatography [6]. Protein concentration and purity were confirmed by Western blotting and Coomassie blue staining. The GFOGER collagen-mimetic peptide was synthesized as previously described [7].

Preparation of micropatterned substrates: micropatterned substrates were generated by microcontact printing of self-assembled monolayers of alkanethiols on gold [8] using a PDMS stamp (Sylgard 184/186 elastomer kit) with circular patterns (10 μm diameter circles, 75 μm center to center spacing). Arrays of methyl-terminated alkanethiol [$HS-(CH_2)_{11}-CH_3$; Sigma] circles were stamped onto Au-coated glass coverslips. The remaining exposed areas were functionalized with a tri(ethylene glycol)-terminated alkanethiol [$HS-(CH_2)_{11}-(CH_2CH_2O)_3-OH$; ProChimia Surfaces] to generate a cell adhesive-resistant background. Patterned substrates were coated with purified adhesive ligands (20 μg/ml), blocked with 1% heat-denatured bovine serum albumin, incubated in PBS (Ca^{2+}/Mg^{2+}), then seeded with cells at a density of 210 cells/mm^2 and incubated for 16 hours at 37˚C.

Cell adhesion assay description: cell adhesion to fibronectin-coated islands was measured using a hydrodynamic spinning disk system [3,4]. Micropatterned substrates with adherent cells were spun in PBS supplemented with 2 mM dextrose for 5 min at constant speeds. The applied shear stress (τ) is given by the formula $\tau = 0.8r(\rho\mu\omega^3)^{1/2}$, where r is the radial position and ρ, μ and ω are the fluid density, viscosity and rotational speed respectively. After spinning, cells were fixed in 3.7% formaldehyde, permeabilized in 1% Triton X-100, stained with ethidium homodimer-1 (Invitrogen). Adherent cells were counted at specific radial positions using a 10X objective lens in a Nikon TE300 microscope equipped with a Ludl motorized stage, Spot-RT camera and an Image-Pro analysis system. A total of 61 fields (80–100 cells per field before spinning) were analyzed and cell counts were normalized to the number of cell counts at the center of the disk. The fraction of adherent cells (f) as a function of shear stress τ (force/area) was then fitted to a sigmoid curve $f = f_0/[1 + \exp[b(\tau - \tau_{50})]]$, where τ_{50} is the shear stress for 50% detachment, b is the inflection slope, and f_0 is the y-intercept. τ_{50} represents the mean adhesion strength for the cell population.

PIP3 Localization Analysis
Adherent cells were serum-starved and paraformaldehyde-fixed following addition of a bolus of EGF (20 ng/mL, 0-60 minutes post stimulation, as indicated). Images were quantified by creating a mask for areas of cell-ECM adhesion based on the vinculin-mEmerald signal. PIP3-probe fluorescence intensity in masked areas was then compared with that in the whole cell to evaluate enrichment of PIP3 at focal adhesions.

Institutional Review Board Information
Cohorts of PyMT and FVB mice were maintained in accordance with University of California IACUC guidelines under protocol AN092125.

References

1. Weaver VM, Petersen OW, Wang F, Larabell CA, Briand P, et al. (1997) Reversion of the malignant phenotype of human breast cells in three-dimensional culture and in vivo by integrin blocking antibodies. J Cell Biol 137: 231–245. Available: http://www.pubmedcentral.nih.gov/articlerender.fcgi?artid=2139858&tool=pmcentrez&rendertype=abstract. Accessed 10 January 2014.

2. Gilbert PM, Mouw JK, Unger MA, Lakins JN, Gbegnon MK, et al. (2010) HOXA9 regulates BRCA1 expression to modulate human breast tumor phenotype. J Clin Invest 120: 1535–1550. Available: http://www.pubmedcentral.nih.gov/articlerender.fcgi?artid=2860938&tool=pmcentrez&rendertype=abstract. Accessed 10 January 2014.

3. Reinhart-King CA, Dembo M, Hammer DA (2003) Endothelial Cell Traction Forces on RGD-Derivatized Polyacrylamide Substrata †. Langmuir 19: 1573–1579. Available: http://dx.doi.org/10.1021/la026142j. Accessed 10 January 2014.

4. Lo C-M, Wang H-B, Dembo M, Wang Y (2000) Cell Movement Is Guided by the Rigidity of the Substrate. Biophys J 79: 144–152. Available: http://www.sciencedirect.com/science/article/pii/S0006349500762795. Accessed 10 January 2014.

5. Radmacher M, Tillamnn R, Fritz M, Gaub H (1992) From molecules to cells: imaging soft samples with the atomic force microscope. Science (80-) 257: 1900–1905. Available: http://www.sciencemag.org/content/257/5078/1900.short. Accessed 10 January 2014.

6. Petrie TA, Capadona JR, Reyes CD, García AJ (2006) Integrin specificity and enhanced cellular activities associated with surfaces presenting a recombinant fibronectin fragment compared to RGD supports. Biomaterials 27: 5459–5470. Available: http://www.ncbi.nlm.nih.gov/pubmed/16846640. Accessed 10 January 2014.

7. Reyes CD, García AJ (2003) Engineering integrin-specific surfaces with a triple-helical collagen-mimetic peptide. J Biomed Mater Res A 65: 511–523. Available: http://www.ncbi.nlm.nih.gov/pubmed/12761842. Accessed 10 January 2014.

8. Gallant ND, Michael KE, García AJ (2005) Cell adhesion strengthening: contributions of adhesive area, integrin binding, and focal adhesion assembly. Mol Biol Cell 16: 4329–4340. Available: http://www.pubmedcentral.nih.gov/articlerender.fcgi?artid=1196341&tool=pmcentrez&rendertype=abstract. Accessed 10 January 2014.